J. Appl. Comput. Mech., 7(2) (2021) 739-751
DOI: 10.22055/JACM.2020.35017.2539

ISSN: 2383-4536
jacm.scu.ac.ir

Shahid Chamran University of Ahvaz

Journal of Applied and Computational Mechanics

Research Paper

Analytical Expressions for the Singularities Treatment in the Three-dimensional Elastostatic Boundary Element Method

Leonardo Fellipe Prado Leite[1], Rodrigo Souza de Melo[2], Fabio Carlos da Rocha[3]

[1] Department of Civil Engineering, Federal University of Sergipe, Avenida Marechal Rondon S/N, São Cristóvão, 49100-000, Brazil, Email: leolvp@academico.ufs.br

[2] Department of Civil Engineering, Federal University of Sergipe, Avenida Marechal Rondon S/N, São Cristóvão, 49100-000, Brazil, Email: djtrylo@academico.ufs.br

[3] Department of Civil Engineering, Federal University of Sergipe, Avenida Marechal Rondon S/N, São Cristóvão, 49100-000, Brazil, Email: fcrocha@ufs.br

Received September 13 2020; Revised November 17 2020; Accepted for publication December 15 2020.
Corresponding author: F.C. da Rocha (fcrocha@ufs.br)

Abstract. The Boundary Element Method (BEM) is one of the most used numerical methods to solve engineering problems. This method has several advantages over other domain methods. However, BEM requires the use of the fundamental solution of the integral formulation that governs the problem under analysis. Furthermore, these fundamental solutions present, in their majority, singular and hyper-singular terms that impair the stability of the numerical solution when the source point is in the element to be integrated. In order to regularize unstable kernels present in the BEM's three-dimensional elastostatic formulation, the present work develops expressions, in Laurent's series, for treatment of the singularity. The precision of the developed expressions is verified on a standard curved triangular element. The results show excellent efficiency in the regularization of singular and hyper-singular kernels for the problem under analysis.

Keywords: Singular kernels, Hyper-singular kernels, Boundary Element Methods, Singularity subtraction technique, Laurent's series.

1. Introduction

The Boundary Element Method (BEM) is one of the principal numerical methods in Science and Engineering. Among its advantages is reducing dimensionality for linear problems and accuracy in solving problems with infinite or semi-infinite domains. Historically, low-order discretization, usually of order one, has been used to model geometries and surface variables. However, recently, there has been increased interest in using higher-order methods to get better accuracy of results with a lesser increase in the computational effort. There are several areas of applications to high-order elements such as acoustics (Canino et al. [1]), electromagnetism (Rjasanow and Weggler [2]), and elasticity (Gao and Davies [3]). The significant difficulty in using high-order BEM is the lack of effective methods for the accurate development of the integrals with singular and hypersingular kernels applied to curved elements.

Among the significant existing integration methods, the Polar Coordinate Transformation (PCT) always serves as a common basis (Guiggiani et al. [4]; Carley [5]; Johnston et al. [6]; Gao [7]). This transformation preserves the surface integral into a double integral in the radial and angular directions. Several studies have been conducted to treat singularity in the radial direction; however, numerical integration in the angular direction merits further attention. Thus, this work shows that after applying the singularity subtraction technique, the kernel in the radial direction is regularized. However, additional care must be considered in the angular direction, such as adopting additional integration points, when the integration domain is distorted. Unfortunately, this case is often found in the use of high-order elements. Another contribution of this paper is the presentation explicit of the Laurent series for the kernels of the three-dimensional BEM integral equations applied to elastostatic problems.

The paper is organized as follows. In section 2, the integral equations of the BEM are presented. In section 3, the treatment of singularity and its applications to the formulation of elastostatic problems is performed. Continuing in section 3, explicit expressions of the Laurent series for three-dimensional elastostatic BEM is presented. Finally, in section 4, the concluding remarks are made.

2. Boundary Integral Equation

There are several ways to get the Boundary Element Method (BEM) formulations, such as by the reciprocity theorem, by concepts of weighted residuals and variational approaches. The BEM formulation to 3D elastostatic problems with source point belonging to the domain is given by (Aliabadi [8]):

Published online: December 16 2020

$$\boldsymbol{u}(\mathrm{Y})=\int_{S}\boldsymbol{U}(\mathrm{Y},\mathrm{x})\cdot\boldsymbol{t}(\mathrm{x})dS-\int_{S}\boldsymbol{T}(\mathrm{Y},\mathrm{x})\cdot\boldsymbol{u}(\mathrm{x})dS+\int_{V}\boldsymbol{U}(\mathrm{Y},\mathrm{X})\cdot\boldsymbol{b}(\mathrm{X})dV, \tag{1}$$

where $\boldsymbol{u}$, $\boldsymbol{t}$, and $\boldsymbol{b}$ are the displacements, tractions, and body forces, respectively. The points X and x represent field values in the domain and on the problem's boundary, respectively, and point Y represents the source point belonging to the domain. In this work, tensor notations $(\boldsymbol{a}\otimes\boldsymbol{b}\otimes\boldsymbol{c})^{321}=(\boldsymbol{c}\otimes\boldsymbol{b}\otimes\boldsymbol{a})$, $\boldsymbol{D}^{312}=D_{kij}\boldsymbol{e}_i\otimes\boldsymbol{e}_j\otimes\boldsymbol{e}_k$, and $\boldsymbol{S}^{312}=S_{kij}\boldsymbol{e}_i\otimes\boldsymbol{e}_j\otimes\boldsymbol{e}_k$ are used. Additionally, throughout the text, the following notation is adopted: zero-order tensor is represented by letters without bold, order one tensor is represented by Latin letters, in bold and lower case. Furthermore, higher-order tensors are represented by capital letters and in bold.

Equation 1 applied to the linear elastic constitutive law (Hooke's law) obtains the integral identity for stress as follows:

$$\sigma(\mathrm{Y})=\int_{S}\boldsymbol{D}^{312}(\mathrm{Y},\mathrm{x})\cdot\boldsymbol{t}(\mathrm{x})dS-\int_{S}\boldsymbol{S}^{312}(\mathrm{Y},\mathrm{x})\cdot\boldsymbol{u}(\mathrm{x})dS+\int_{V}\boldsymbol{D}^{312}(\mathrm{Y},\mathrm{x})\cdot\boldsymbol{b}(\mathrm{X})dV. \tag{2}$$

Moreover, the terms $\boldsymbol{U}(\mathrm{Y},\mathrm{x})$, $\boldsymbol{T}(\mathrm{Y},\mathrm{x})$, $\boldsymbol{D}(\mathrm{Y},\mathrm{x})$, and $\boldsymbol{S}(\mathrm{Y},\mathrm{x})$ are called fundamental solutions and are shown by (Aliabadi [8]):

$$\boldsymbol{U}(\mathrm{Y},\mathrm{x})=\frac{1}{16\pi\mu(1-\nu)r}\left[(3-4\nu)\boldsymbol{I}+\hat{\boldsymbol{r}}\otimes\hat{\boldsymbol{r}}\right]; \tag{3}$$

$$\boldsymbol{T}(\mathrm{Y},\mathrm{x})=-\frac{1}{8\pi(1-\nu)r^2}\left\{(\boldsymbol{n}\cdot\nabla r)\left[(1-2\nu)\boldsymbol{I}+3\hat{\boldsymbol{r}}\otimes\hat{\boldsymbol{r}}\right]+(1-2\nu)(\boldsymbol{n}\otimes\hat{\boldsymbol{r}}-\hat{\boldsymbol{r}}\otimes\boldsymbol{n})\right\}; \tag{4}$$

$$\boldsymbol{D}^{312}(\mathrm{Y},\mathrm{x})=\frac{1}{8\pi(1-\nu)r^2}\left\{(1-2\nu)\left[(\boldsymbol{I}\otimes\hat{\boldsymbol{r}})+(\boldsymbol{I}\otimes\hat{\boldsymbol{r}})^{132}-(\hat{\boldsymbol{r}}\otimes\boldsymbol{I})\right]+3\hat{\boldsymbol{r}}\otimes\hat{\boldsymbol{r}}\otimes\hat{\boldsymbol{r}}\right\}; \tag{5}$$

$$\boldsymbol{S}^{312}(\mathrm{Y},\mathrm{x})=\frac{1}{4\pi(1-\nu)r^3}\left\{\begin{array}{l}3(\boldsymbol{n}\cdot\hat{\boldsymbol{r}})\left[(1-2\nu)\hat{\boldsymbol{r}}\otimes\boldsymbol{I}+\nu\left[(\boldsymbol{I}\otimes\hat{\boldsymbol{r}})^{213}+(\boldsymbol{I}\otimes\hat{\boldsymbol{r}})^{312}\right]-5\hat{\boldsymbol{r}}\otimes\hat{\boldsymbol{r}}\otimes\hat{\boldsymbol{r}}\right]\\ +3\nu(\hat{\boldsymbol{r}}\otimes\boldsymbol{n}\otimes\hat{\boldsymbol{r}}+\hat{\boldsymbol{r}}\otimes\hat{\boldsymbol{r}}\otimes\boldsymbol{n})+(1-2\nu)\left[\begin{array}{l}3\boldsymbol{n}\otimes\hat{\boldsymbol{r}}\otimes\hat{\boldsymbol{r}}+(\boldsymbol{I}\otimes\boldsymbol{n})^{213}\\+(\boldsymbol{I}\otimes\boldsymbol{n})^{312}\end{array}\right]\\ -(1-4\nu)\boldsymbol{n}\otimes\boldsymbol{I}\end{array}\right\}. \tag{6}$$

where r, ν, E and $\mu=E/2(1+\upsilon)$ is the distance between the field point and the source point, Poisson's ratio, Young's modulus and shear modulus of elasticity, respectively. $\hat{\boldsymbol{r}}=\boldsymbol{r}/r$ is unit distance vector. $\boldsymbol{n}$ is normal vector and $\boldsymbol{I}$ is second order identity tensor.

The boundary integral equations for displacement (1) and stress (2) are valid for any source point within the domain V. For the source point on the boundary, S, it is necessary to consider the limit $Y\to y$ and $y\in S$. The process is carried out by considering a semi-circular region surrounding the source point y, such that the new boundary region S^A is given by

$$S^A=(S-S_{\epsilon})+S_{\epsilon}^{+}. \tag{7}$$

Here S_{ϵ} is the portion of the original boundary removed, and S_{ϵ}^{+} is the portion inserted to this boundary. The singularity behavior is studied considering the limit $\epsilon\to 0$ and, therefore, $S^A\to S$. Thus, performing the limit analysis (Aliabadi, 2002), one can write:

$$\boldsymbol{C}(\mathrm{y})\cdot\boldsymbol{u}(\mathrm{y})+\lim_{\epsilon\to 0}\left\{\int_{S-S_{\epsilon}}\left[\boldsymbol{T}(\mathrm{y},\mathrm{x})\cdot\boldsymbol{u}(\mathrm{x})-\boldsymbol{U}(\mathrm{y},\mathrm{x})\cdot\boldsymbol{t}(\mathrm{x})\right]dS\right\}-\int_{V}\boldsymbol{U}(\mathrm{y},\mathrm{X})\cdot\boldsymbol{b}(\mathrm{X})dV=0; \tag{8}$$

$$\bar{\boldsymbol{C}}(\mathrm{y}):\boldsymbol{\sigma}(\mathrm{y})+\lim_{\epsilon\to 0}\left\{\int_{S-S_{\epsilon}}\left[\boldsymbol{S}^{312}(\mathrm{y},\mathrm{x})\cdot\boldsymbol{u}(\mathrm{x})-\boldsymbol{D}^{312}(\mathrm{y},\mathrm{x})\cdot\boldsymbol{t}(\mathrm{x})+\boldsymbol{u}(\mathrm{y})\cdot\frac{\boldsymbol{B}^{312}(\mathrm{y})}{\epsilon}\right]dS\right\}-\int_{V}\boldsymbol{D}^{312}(\mathrm{y},\mathrm{X})\cdot\boldsymbol{b}(\mathrm{X})dV=0; \tag{9}$$

where the tensor $\boldsymbol{C}(\mathrm{y})$, $\bar{\boldsymbol{C}}(\mathrm{y})$, and $\boldsymbol{B}^{312}(\mathrm{y})$ are coefficients (limited) that depend only on the local geometry S in y. If y is a smooth boundary point and S_{ϵ} has a circular shape, the free terms $\boldsymbol{C}(\mathrm{y})$ and $\bar{\boldsymbol{C}}(\mathrm{y})$ in Eqs (8) and (9) are reduced to $0{,}5\boldsymbol{I}$ and $0{,}5\bar{\boldsymbol{I}}(=0{,}5\delta_{ij}\delta_{th})$.

The singularity's level of kernels of the boundary integral equations in Eq (1) and (2) can be defined as (Gao [7])

$$\left\{\begin{array}{cc}\beta\le 0, & \text{regular}\\ 0<\beta\le D-1 & \text{weakly singular}\\ \beta=D-1 & \text{strongly singular},\\ \beta=D & \text{hypersingular}\\ \beta>D & \text{supersingular}\end{array}\right. \tag{10}$$

where D is the Cartesian dimension (in this work $D=3$), and β is the exponent that accompanies the distance between the field point and source point, $(f(\mathrm{y},\mathrm{x})/r^{\beta})$. Thus, according to Eq. (10), Eq. (6) is classified as weakly singular, Eq. (4)-(5) are strongly singular and Eq. (6) is hypersingular.

3. Development of Numerical Integral Equation

The numerical evolution of hypersingular, weakly, and strongly singular equations is performed in this section.

3.1 Treatment of singularities in BEM integral equations

This subsection shows the singularity's treatment to regularize the integral equations (8) and (9). However, without loss of generality, the hypersingular equation analysis is performed, since the other cases of singularity are obtained as particularities. This way, one has as aim the development of limited quantity, present in the Eq. (9),

$$\lim_{\in\to 0}\left\{\int_{S-S_\in}\left[\boldsymbol{S}^{312}(y,x)\cdot\boldsymbol{u}(x)-\boldsymbol{D}^{312}(y,x)\cdot\boldsymbol{t}(x)+\boldsymbol{u}(y)\cdot\frac{\boldsymbol{B}^{312}(y)}{\in}\right]dS\right\}, \tag{11}$$

is calculated in the neighborhood $S_\in$, around the source point y in S, given by

$$S_\in=\{x\in S\,\|\,x-y\,|\leq\in\}. \tag{12}$$

Equation (11) can be split into two sets of integral, such that in this section, the portion corresponding to the hyper-singular kernel is developed

$$\lim_{\in\to 0}\left\{\int_{S-S_\in}\left[\boldsymbol{S}^{312}(y,x)\cdot\boldsymbol{u}(x)+\boldsymbol{u}(y)\cdot\frac{\boldsymbol{B}^{312}(y)}{\in}\right]dS\right\}, \tag{13}$$

where $\boldsymbol{S}^{312}=O(r^{-3})$.

The other term of Eq. (11) is calculated as a particular case the procedure here briefly presented.

As usual, in each boundary element, the displacements are represented by the shape functions $N^a(\xi_1,\xi_2)$ with dimensionless local coordinate $\boldsymbol{\xi}=(\xi_1,\xi_2)$. Thus the displacements are approximated by $\boldsymbol{u}(x)=\sum_{a=1}^{A(e)}N^a[\boldsymbol{\xi}(x)]\boldsymbol{u}_e^a$, with $A(e)$ being the number of nodes in the element. . Therefore, the secondary aim results in the calculation of integral I defined on an element(s) S_S

$$I=\lim_{\in\to 0}\left\{\int_{S_S-S_\in}\left[S_{kij}(y,x)N^a[\boldsymbol{\xi}(x)]+N^a[\boldsymbol{\eta}]\frac{b_{kij}(y)}{\in}\right]dS\right\}, \tag{14}$$

where S_S is denoted as the region into S containing the singular point y.

Following, Guiggiani et al. [4] carry out polar coordinate transformation (PCT) in Eq. (14). The PCT, (ρ,θ), is centered at $\boldsymbol{\eta}$ (image of y) and is defined in the parameter plane

$$\begin{cases}\xi_1=\eta_1+\rho\cos\theta\\ \xi_2=\eta_2+\rho sen\theta\end{cases}. \tag{15}$$

The substitution of Eq. (15) in Eq. (14) allows writing the equation

$$I=\lim_{\in\to 0}\left\{\int_0^{2\pi}\int_{\alpha(\in,\theta)}^{\hat\rho(\theta)}F(\rho,\theta)d\rho d\theta+N^a[\boldsymbol{\eta}]\frac{b_{kij}(y)}{\in}\right\}, \tag{16}$$

with $F(\rho,\theta)=S_{kij}(y,x(\rho,\theta))N^a(\rho,\theta)J(\rho,\theta)\equiv O(\rho^{-2})$, $\rho=\alpha(\in,\theta)$ being a polar coordinate equation to $\sigma_\in$ (see Fig. 1). Furthermore, $\rho=\hat\rho(\theta)$ being a polar coordinate equation of the outer boundary in the parametric domain R_S (see Fig. 1).

For the analysis of the singular function $F(\rho,\theta)$ of order ρ^{-2}, expansions in Laurent series concerning ρ are used, such as

$$F(\rho,\theta)=\frac{F_{-2}(\theta)}{\rho^2}+\frac{F_{-1}(\theta)}{\rho}+O(1). \tag{17}$$

Note that F_{-2} as well as F_{-1} are dependent only on θ. This series expansion is the key point to the subtraction of singularity.

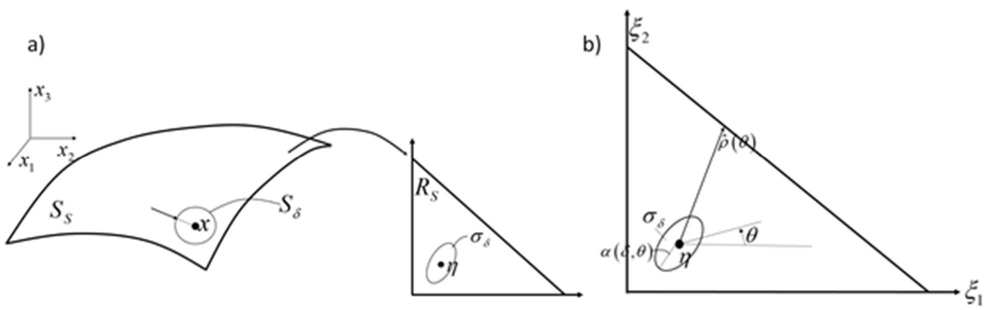

Fig. 1. (a) the image in the parametric plane of both the boundary element and the region with subtracted singularity. (b) parametric plane in polar coordinate.

Another series expansion is performed in the region bounded by $\alpha(\in,\theta)$, i.e., the Taylor series expansion concerning the $\in$ is written as:

$$\rho = \alpha(\in,\theta) = \in \beta(\theta) + \in^2 \gamma(\theta) + O(\in^3). \tag{18}$$

It can be observed in general that $\rho = \in \beta(\theta)$ is the equation of an ellipse.

In the next section, the development to obtain the explicit expressions to F_{-1}, F_{-2}, $\beta(\theta)$, and $\gamma(\theta)$ for three-dimensional elastostatic problems has been presented. However, at present, it is made semi-analytical treatment of Eq. (16). This treatment is carried out utilizing an algebraic manipulation that consists of adding and subtracting the first two terms of expanding the series (17) in Eq (16), thus obtaining:

$$\begin{aligned} I &= \lim_{\in\to 0}\left\{\int_0^{2\pi}\int_{\alpha(\in,\theta)}^{\hat{\rho}(\theta)}\left[F(\rho,\theta)-\left(\frac{F_{-2}(\theta)}{\rho^2}+\frac{F_{-1}(\theta)}{\rho}\right)\right]d\rho d\theta+\int_0^{2\pi}\int_{\alpha(\in,\theta)}^{\hat{\rho}(\theta)}\frac{F_{-1}(\theta)}{\rho}d\rho d\theta+\int_0^{2\pi}\int_{\alpha(\in,\theta)}^{\hat{\rho}(\theta)}\frac{F_{-2}(\theta)}{\rho^2}d\rho d\theta+N^a[\eta]\frac{b_{kij}(y)}{\in}\right\} \\ I &= I_0 + I_{-1} + I_{-2}. \end{aligned} \tag{19}$$

Each term of Eq. (19) is analyzed separately, and the following expressions are obtained (Guiggiani et al. [4]):

$$I_0 = \int_0^{2\pi}\int_0^{\hat{\rho}(\theta)}\left[F(\rho,\theta)-\left(\frac{F_{-2}(\theta)}{\rho^2}+\frac{F_{-1}(\theta)}{\rho}\right)\right]d\rho d\theta. \tag{20}$$

$$I_{-1} = \int_0^{2\pi} F_{-1}(\theta)\ln\left|\frac{\hat{\rho}(\theta)}{\beta(\theta)}\right|d\theta. \tag{21}$$

$$I_{-2} = -\int_0^{2\pi} F_{-2}(\theta)\left[\frac{\gamma(\theta)}{\beta^2(\theta)}+\frac{1}{\hat{\rho}(\theta)}\right]d\theta. \tag{22}$$

where $\beta(\theta)$ and $\gamma(\theta)$ are coefficients of the series expansion given by Eq. (18). While the term $\hat{\rho}(\theta)$ represents the polar coordinate of the outer boundary in R_S (see Fig. 1).

If the singular point belongs to more than one element, i.e. $S_S = \bigcup_{i=1}^{m} S_i$, then the final formula for singularity treatment is:

$$I = \sum_{i=1}^{m}\left\{\int_{\theta_1^i}^{\theta_2^i}\int_0^{\hat{\rho}^i(\theta)}\left[F^i(\rho,\theta)-\left(\frac{F^i_{-2}(\theta)}{\rho^2}+\frac{F^i_{-1}(\theta)}{\rho}\right)\right]d\rho d\theta+\int_{\theta_1^i}^{\theta_2^i}F^i_{-1}(\theta)\ln\left|\frac{\hat{\rho}^i(\theta)}{\beta^i(\theta)}\right|d\theta-\int_{\theta_1^i}^{\theta_2^i}F^i_{-2}(\theta)\left[\frac{\gamma^i(\theta)}{\left(\beta^2(\theta)\right)^i}+\frac{1}{\hat{\rho}^i(\theta)}\right]d\theta\right\}, \tag{23}$$

with the i-th index refers to each element around the placement point and $\theta_1^i \le \theta \le \theta_2^i$ in the i-th element.

The formula (23) is entirely general. This formula can be used for any element and on integrals with a lower classification of singularity. For example, if the integrals' kernel is only strongly singular, then Laurent expansion (17) has $F_{-2}(\theta)=0$ in the final formula (23). Another possibility is when the integral kernel is only weakly singular, so it follows that $F_{-1}(\theta)=0$ and $F_{-2}(\theta)=0$ in Eq. (23).

3.2 Application of the singularity treatment to three-dimensional elastostatic problems

As is already known, only for some elementary problems, Eq. (8) and Eq. (9) can be solved analytically. In this way, the search for numerical solutions becomes essential. Here, the smooth surface S_S is discretized into N_e isoparametric high-order triangular elements with $A(e)$ representing the number of nodes per element. The source point, y, is considered in the S_S contour in addition to the hypothesis of absence of body force. For simplicity, the global numbering for the nodes is associated with the ς number. Thus, by performing the singularity subtraction using Eq (23), the BEM integral equations for 3D elastostatic problems are written in the following form for nodal point k:

$$\begin{aligned} \frac{1}{2}\boldsymbol{u}^k + \sum_{\varsigma=1}^{L}\boldsymbol{H}_\varsigma^k\cdot u^\varsigma &= \sum_{\varsigma=1}^{L}\boldsymbol{G}_\varsigma^k\cdot P^z \\ \frac{1}{2}\sigma^k + \sum_{\varsigma=1}^{L}\bar{\boldsymbol{H}}_\varsigma^k\cdot u^\varsigma &= \sum_{\varsigma=1}^{L}\bar{\boldsymbol{G}}_\varsigma^k\cdot P^z \end{aligned}.$$

where L is the total number of nodes and

$$\boldsymbol{G}_\varsigma^k = \int_{\theta_1}^{\theta_2}\int_0^{\hat{\rho}(\theta)}\tilde{\boldsymbol{K}}(\rho,\theta)d\rho d\theta\,, \tag{24}$$

$$\boldsymbol{H}_\varsigma^k = \int_{\theta_1}^{\theta_2}\int_0^{\hat{\rho}(\theta)}\left[\tilde{\boldsymbol{W}}(\rho,\theta)-\frac{\tilde{\boldsymbol{W}}_{-1}(\theta)}{\rho}\right]d\rho d\theta+\int_{\theta_1}^{\theta_2}\tilde{\boldsymbol{W}}_{-1}(\theta)\ln\left|\frac{\hat{\rho}(\theta)}{\beta(\theta)}\right|d\theta\,, \tag{25}$$

$$\bar{\boldsymbol{H}}_\varsigma^k = \int_{\theta_1}^{\theta_2}\int_0^{\hat{\rho}(\theta)}\left[\tilde{\boldsymbol{D}}(\rho,\theta)-\frac{\tilde{\boldsymbol{D}}_{-1}(\theta)}{\rho}\right]d\rho d\theta+\int_{\theta_1}^{\theta_2}\tilde{\boldsymbol{D}}_{-1}(\theta)\ln\left|\frac{\hat{\rho}(\theta)}{\beta(\theta)}\right|d\theta\,, \tag{26}$$

$$\tilde{G}_{\varsigma}^{k} = \int_{\theta_1}^{\theta_2}\int_{0}^{\hat{\rho}(\theta)}\left[\tilde{S}(\rho,\theta)-\left(\frac{\tilde{S}_{-2}(\theta)}{\rho^2}+\frac{\tilde{S}_{-1}(\theta)}{\rho}\right)\right]d\rho d\theta + \int_{\theta_1}^{\theta_2}\left\{\tilde{S}_{-1}(\theta)\ln\left|\frac{\hat{\rho}(\theta)}{\beta(\theta)}\right| - \tilde{S}_{-2}(\theta)\left[\frac{\gamma(\theta)}{\beta^2(\theta)}+\frac{1}{\hat{\rho}(\theta)}\right]\right\}d\theta . \tag{27}$$

where $\tilde{K}(\rho,\theta)$, $\tilde{W}(\rho,\theta)$, $\tilde{D}(\rho,\theta)$ and $\tilde{S}(\rho,\theta)$ are presented in polar coordinates:

$$\tilde{K}(\rho,\theta) = U\left(y^k, x(\rho,\theta)\right)N^a(\rho,\theta)J(\rho,\theta) , \tag{28}$$

$$\tilde{W}(\rho,\theta) = T\left(y^k, x(\rho,\theta)\right)N^a(\rho,\theta)J(\rho,\theta) , \tag{29}$$

$$\tilde{D}(\rho,\theta) = D^{312}\left(y^k, x(\rho,\theta)\right)N^a(\rho,\theta)J(\rho,\theta) , \tag{30}$$

$$\tilde{S}(\rho,\theta) = S^{312}\left(y^k, x(\rho,\theta)\right)N^a(\rho,\theta)J(\rho,\theta) . \tag{31}$$

In the next section, all parameters of Eq. (25)-(31) are explained.

3.3 Explicit expressions of Laurent series and of $\beta(\theta)$ and $\gamma(\theta)$ parameters to 3D elastostatic BEM problems

Before starting the procedure for obtaining the terms $\tilde{W}_{-1}(\theta)$, $\tilde{D}_{-1}(\theta)$, $\tilde{D}_{-2}(\theta)$, $\tilde{S}_{-1}(\theta)$, $\tilde{S}_{-2}(\theta)$, $\beta(\theta)$ and $\gamma(\theta)$, some Taylor series expansions must be made around the source point $y \in S_S$.

As routinely performed in BEM, the coordinates of a generic point on the contour element, S_S, are given by parametric representation in terms of shape functions $M^c(\xi_1,\xi_2)$ and nodal coordinates x^c,

$$x = \sum_{c=1}^{k} M^c(\xi_1,\xi_2)x^c. \tag{32}$$

The image of the source point, y, is indicated by $\eta = (\eta_1,\eta_2)$, such that

$$y = \sum_{c=1}^{k} M^c(\eta_1,\eta_2)x^c. \tag{33}$$

From Eq. (32), the first and second derivatives are obtained by

$$\frac{\partial x}{\partial \xi_t} = \sum_{c=1}^{k}\frac{\partial M^c(\xi_1,\xi_2)}{\partial \xi_t}x^c, \quad t = 1,2, \tag{34}$$

$$\frac{\partial^2 x}{\partial \xi_t^2} = \sum_{c=1}^{k}\frac{\partial^2 M^c(\xi_1,\xi_2)}{\partial \xi_t^2}x^c, \quad t = 1,2. \tag{35}$$

The Taylor series in polar coordinates for the difference between the field point and the source point can be written as

$$x(\xi_1,\xi_2) - y(\eta_1,\eta_2) = \rho\left[\left.\frac{\partial x}{\partial \xi_1}\right|_{\xi=\eta}(\cos\theta) + \left.\frac{\partial x}{\partial \xi_2}\right|_{\xi=\eta}(sen\theta)\right] + \rho^2\left[\left.\frac{\partial^2 x}{\partial \xi_1^2}\right|_{\xi=\eta}\frac{(\cos\theta)^2}{2} + \left.\frac{\partial^2 x}{\partial \xi_1\partial \xi_2}\right|_{\xi=\eta}(\cos\theta)(sen\theta) + \left.\frac{\partial^2 x}{\partial \xi_2^2}\right|_{\xi=\eta}\frac{(sen\theta)^2}{2}\right] + O(\rho^3), \tag{36}$$

or abbreviated,

$$x(\xi_1,\xi_2) - y(\eta_1,\eta_2) = \rho A(\theta) + \rho^2 B(\theta) + O(\rho^3). \tag{37}$$

Then, the scalars are defined

$$A(\theta) = |A(\theta)| = \sqrt{\sum_{k=1}^{3}[A_k(\theta)]^2} > 0, \tag{38}$$

$$B(\theta) = |B(\theta)| = \sqrt{\sum_{k=1}^{3}[B_k(\theta)]^2} \geq 0. \tag{39}$$

According to the above results, the Taylor series expansions for the power of the radius is given by

$$r^n = |r|^n = \rho^n A^n\left[1 + n\rho\frac{(A\cdot B)}{A^2}\right] + O(\rho^{n+2}), \quad n = 1,2,3\ldots. \tag{40}$$

For developments that follow are required to reverse series, i.e., calculating the coefficients of the inverse series with and without the constant term. For this, we consider the generic power series $Z = \sum_{n=i}^{\infty} z_n X^n$ in which its inverse is represented by $G = \sum_{n=i}^{\infty} g_n X^n$ series with coefficients, g_n, calculated considering $i = 0$ and $i = 1$, i.e., with and without the constant term is given (Abramowitz and Stegun [9]), respectively, by Eq. (41)

$$g_0 = \frac{1}{z_0}, \quad g_t = -\frac{1}{z_0}\sum_{i=1}^{t} z_i g_{t-i} \tag{41}$$

and Eq. (42)

$$g_1 = \frac{1}{z_1}, \quad g_2 = -\frac{z_2}{z_1^{\ 3}}, \quad g_3 = \frac{2z_2^{\ 2}}{z_1^{\ 5}} \ldots \tag{42}$$

From Eq. (38)-(41) with $n = 1$, the expressions for $\hat{\boldsymbol{r}} = \boldsymbol{r} / r$ are obtained by:

$$\hat{\boldsymbol{r}} = \frac{\boldsymbol{r}}{r} = \frac{\boldsymbol{A}(\theta)}{\mathrm{A}(\theta)} + \rho\left[\frac{\boldsymbol{B}(\theta)}{\mathrm{A}(\theta)} - \boldsymbol{A}(\theta)\frac{(\boldsymbol{A}(\theta)\cdot\boldsymbol{B}(\theta))}{\mathrm{A}^3(\theta)}\right] + \mathrm{O}(\rho^2) = \boldsymbol{d}_0(\theta) + \rho\boldsymbol{d}_1(\theta) + \mathrm{O}(\rho^2) \tag{43}$$

The series expansion for r^{-n} is of great importance. This expansion is obtained using Eq.(40) and (41), as shown in Eq. (44).

$$\frac{1}{|\boldsymbol{r}|^n} = \frac{1}{\rho^n \mathrm{A}^n} - n\frac{(\boldsymbol{A}(\theta)\cdot\boldsymbol{B}(\theta))}{\rho^{n-1}\mathrm{A}^{n+2}(\theta)} + \mathrm{O}\left(\frac{1}{\rho^{n-2}}\right), \quad n = 1,2,3\ldots \tag{44}$$

The other expansions of the Taylor series that will be used to build the Laurent series are the expansions of the shape functions, Jacobian, Jacobian module, normal vector (concerning the field point), which are presented, respectively, by Eq. (45)-(49)

$$\mathrm{N}^a(\xi) = \mathrm{N}^a(\eta) + \rho\left[\left.\frac{\partial \mathrm{N}^a}{\partial \xi_1}\right|_{\xi=\eta}\cos\theta + \left.\frac{\partial \mathrm{N}^a}{\partial \xi_2}\right|_{\xi=\eta} sen\theta\right] + \mathrm{O}(\rho^2) = \mathrm{N}_0^a + \rho\mathrm{N}_1^a(\theta) + \mathrm{O}(\rho^2), \tag{45}$$

$$\boldsymbol{J}(\xi) = \boldsymbol{J}(\eta) + \rho\left[\left.\frac{\partial \boldsymbol{J}(\xi)}{\partial \xi_1}\right|_{\xi=\eta}\cos\theta + \left.\frac{\partial \boldsymbol{J}(\xi)}{\partial \xi_2}\right|_{\xi=\eta} sen\theta\right] + \mathrm{O}(\rho^2) = \boldsymbol{J}_0 + \rho\boldsymbol{J}_1(\theta) + \mathrm{O}(\rho^2), \tag{46}$$

$$J = |\boldsymbol{J}| = \left\{\textstyle\sum_{k=1}^3 J_k^2\right\}^{1/2} = |\boldsymbol{J}_0| + \rho\frac{(\boldsymbol{J}_0\cdot\boldsymbol{J}_1)}{|\boldsymbol{J}_0|} + \mathrm{O}(\rho^2) = J_0 + \rho J_1(\theta) + \mathrm{O}(\rho^2), \tag{47}$$

with

$$\begin{aligned} J_0 &= |\boldsymbol{J}_0| = \sqrt{\textstyle\sum_{k=1}^3 J_{k0}^2} \\ J_1(\theta) &= \frac{(J_{k0}\cdot J_{k1})}{|\boldsymbol{J}_0|} \end{aligned} \tag{48}$$

$$\boldsymbol{n} = \frac{\boldsymbol{J}}{J} = \frac{\boldsymbol{J}_0}{J_0} + \rho\left[\frac{\boldsymbol{J}_1(\theta)}{J_0} - \boldsymbol{J}_1(\theta)\frac{J_1(\theta)}{J_0^2}\right] + \mathrm{O}(\rho^2) = \hat{\boldsymbol{n}}^0 + \rho\hat{\boldsymbol{n}}^1(\theta) + \mathrm{O}(\rho^2). \tag{49}$$

From Eq. (3)-(6), some results of tensor algebra must be expanded in series. Such expansions are

$$\begin{aligned} \hat{\boldsymbol{r}}\otimes\hat{\boldsymbol{r}} &= \boldsymbol{d}_0(\theta)\otimes\boldsymbol{d}_0(\theta) + \rho(\boldsymbol{d}_1(\theta)\otimes\boldsymbol{d}_0(\theta) + \boldsymbol{d}_0(\theta)\otimes\boldsymbol{d}_1(\theta)) + \mathrm{O}(\rho^2) \\ &= (\hat{\boldsymbol{r}}\otimes\hat{\boldsymbol{r}})_0 + \rho(\hat{\boldsymbol{r}}\otimes\hat{\boldsymbol{r}})_1 + \mathrm{O}(\rho^2), \end{aligned} \tag{50}$$

$$\begin{aligned} \boldsymbol{n}\otimes\hat{\boldsymbol{r}} &= \boldsymbol{n}^0\otimes\boldsymbol{d}_0(\theta) + \rho\left[\boldsymbol{n}^0\otimes\boldsymbol{d}_1(\theta) + \boldsymbol{n}^1(\theta)\otimes\boldsymbol{d}_0(\theta)\right] + \mathrm{O}(\rho^2) \\ &= (\boldsymbol{n}\otimes\hat{\boldsymbol{r}})_0 + \rho(\boldsymbol{n}\otimes\hat{\boldsymbol{r}})_1 + \mathrm{O}(\rho^2), \end{aligned} \tag{51}$$

$$\begin{aligned} \hat{\boldsymbol{r}}\otimes\boldsymbol{n} &= \boldsymbol{d}_0(\theta)\otimes\boldsymbol{n}^0 + \rho\left[\boldsymbol{d}_0(\theta)\otimes\boldsymbol{n}^1(\theta) + \boldsymbol{d}_1(\theta)\otimes\boldsymbol{n}^0\right] \\ &= (\hat{\boldsymbol{r}}\otimes\boldsymbol{n})_0 + \rho(\hat{\boldsymbol{r}}\otimes\boldsymbol{n})_1 + \mathrm{O}(\rho^2), \end{aligned} \tag{52}$$

$$\begin{aligned} \boldsymbol{n} = \boldsymbol{I}\otimes\hat{\boldsymbol{r}} &= \boldsymbol{I}\otimes\boldsymbol{d}_0(\theta) + \rho(\boldsymbol{I}\otimes\boldsymbol{d}_1(\theta)) + \mathrm{O}(\rho^2) \\ &= (\boldsymbol{I}\otimes\hat{\boldsymbol{r}})_0 + \rho(\boldsymbol{I}\otimes\hat{\boldsymbol{r}})_1 + \mathrm{O}(\rho^2), \end{aligned} \tag{53}$$

$$\begin{aligned} (\boldsymbol{I}\otimes\hat{\boldsymbol{r}})^{132} &= \left[\boldsymbol{I}\otimes\boldsymbol{d}_0(\theta)\right]^{132} + \rho\left[\boldsymbol{I}\otimes\boldsymbol{d}_1(\theta)\right]^{132} + \mathrm{O}(\rho^2) \\ &= (\boldsymbol{I}\otimes\hat{\boldsymbol{r}})_0^{132} + \rho(\boldsymbol{I}\otimes\hat{\boldsymbol{r}})_1^{132} + \mathrm{O}(\rho^2), \end{aligned} \tag{54}$$

$$\begin{aligned} (\boldsymbol{I}\otimes\hat{\boldsymbol{r}})^{213} &= \left[\boldsymbol{I}\otimes\boldsymbol{d}_0(\theta)\right]^{213} + \rho\left[\boldsymbol{I}\otimes\boldsymbol{d}_1(\theta)\right]^{213} + \mathrm{O}(\rho^2) \\ &= (\boldsymbol{I}\otimes\hat{\boldsymbol{r}})_0^{213} + \rho(\boldsymbol{I}\otimes\hat{\boldsymbol{r}})_1^{213} + \mathrm{O}(\rho^2), \end{aligned} \tag{55}$$

$$
\begin{aligned}
(\boldsymbol{I}\otimes\hat{\boldsymbol{r}})^{312} &= [\boldsymbol{I}\otimes\boldsymbol{d}_0(\theta)]^{312}+\rho[\boldsymbol{I}\otimes\boldsymbol{d}_1(\theta)]^{312}+\mathrm{O}(\rho^2)\\
&=(\boldsymbol{I}\otimes\hat{\boldsymbol{r}})_0^{312}+\rho(\boldsymbol{I}\otimes\hat{\boldsymbol{r}})_1^{312}+\mathrm{O}(\rho^2),
\end{aligned}
\tag{56}
$$

$$
\begin{aligned}
(\hat{\boldsymbol{r}}\otimes\boldsymbol{I}) &= \boldsymbol{d}_0(\theta)\otimes\boldsymbol{I}+\rho(\boldsymbol{d}_1(\theta)\otimes\boldsymbol{I})+\mathrm{O}(\rho^2)\\
&=(\hat{\boldsymbol{r}}\otimes\boldsymbol{I})_0+\rho(\hat{\boldsymbol{r}}\otimes\boldsymbol{I})_1+\mathrm{O}(\rho^2),
\end{aligned}
\tag{57}
$$

$$
\begin{aligned}
(\boldsymbol{n}\cdot\hat{\boldsymbol{r}}) &= \boldsymbol{n}^0\cdot\boldsymbol{d}_0(\theta)+\rho[\boldsymbol{n}^0\cdot\boldsymbol{d}_1(\theta)+\boldsymbol{n}^1\cdot\boldsymbol{d}_0(\theta)]+\mathrm{O}(\rho^2)\\
&=\rho[\boldsymbol{n}^0\cdot\boldsymbol{d}_1(\theta)+\boldsymbol{n}^1\cdot\boldsymbol{d}_0(\theta)]+\mathrm{O}(\rho^2)=\rho(\hat{\boldsymbol{n}}_x\cdot\hat{\boldsymbol{r}})_1+\mathrm{O}(\rho^2),
\end{aligned}
\tag{58}
$$

$$
\begin{aligned}
\hat{\boldsymbol{r}}\otimes\hat{\boldsymbol{r}}\otimes\hat{\boldsymbol{r}} &= \boldsymbol{d}_0(\theta)\otimes\boldsymbol{d}_0(\theta)\otimes\boldsymbol{d}_0(\theta)+\rho\begin{Bmatrix}\boldsymbol{d}_0(\theta)\otimes\boldsymbol{d}_0(\theta)\otimes\boldsymbol{d}_1(\theta)+\boldsymbol{d}_0(\theta)\otimes\boldsymbol{d}_1(\theta)\otimes\boldsymbol{d}_0(\theta)\\+\boldsymbol{d}_1(\theta)\otimes\boldsymbol{d}_0(\theta)\otimes\boldsymbol{d}_0(\theta)\end{Bmatrix}+\mathrm{O}(\rho^2)\\
&=(\hat{\boldsymbol{r}}\otimes\hat{\boldsymbol{r}}\otimes\hat{\boldsymbol{r}})_0+\rho(\hat{\boldsymbol{r}}\otimes\hat{\boldsymbol{r}}\otimes\hat{\boldsymbol{r}})_1+\mathrm{O}(\rho^2),
\end{aligned}
\tag{59}
$$

$$
\begin{aligned}
\hat{\boldsymbol{r}}\otimes\mathrm{n}\otimes\hat{\boldsymbol{r}} &= \boldsymbol{d}_0(\theta)\otimes\hat{\boldsymbol{n}}^0\otimes\boldsymbol{d}_0(\theta)+\rho\begin{bmatrix}\boldsymbol{d}_0(\theta)\otimes\hat{\boldsymbol{n}}^0\otimes\boldsymbol{d}_1(\theta)+\boldsymbol{d}_0(\theta)\otimes\hat{\boldsymbol{n}}^1(\theta)\otimes\boldsymbol{d}_0(\theta)\\+\boldsymbol{d}_1(\theta)\otimes\hat{\boldsymbol{n}}^0\otimes\boldsymbol{d}_0(\theta)\end{bmatrix}+\mathrm{O}(\rho^2)\\
&=(\hat{\boldsymbol{r}}\otimes\mathrm{n}\otimes\hat{\boldsymbol{r}})_0+\rho(\hat{\boldsymbol{r}}\otimes\mathrm{n}\otimes\hat{\boldsymbol{r}})_1+\mathrm{O}(\rho^2),
\end{aligned}
\tag{60}
$$

$$
\begin{aligned}
\hat{\boldsymbol{r}}\otimes\hat{\boldsymbol{r}}\otimes\mathrm{n} &= \boldsymbol{d}_0(\theta)\otimes\boldsymbol{d}_0(\theta)\otimes\hat{\boldsymbol{n}}^0+\rho\begin{bmatrix}\boldsymbol{d}_0(\theta)\otimes\boldsymbol{d}_0(\theta)\otimes\hat{\boldsymbol{n}}^1(\theta)+\boldsymbol{d}_0(\theta)\otimes\boldsymbol{d}_1(\theta)\otimes\hat{\boldsymbol{n}}^0\\+\boldsymbol{d}_1(\theta)\otimes\boldsymbol{d}_0(\theta)\otimes\hat{\boldsymbol{n}}^0\end{bmatrix}+\mathrm{O}(\rho^2)\\
&=(\hat{\boldsymbol{r}}\otimes\hat{\boldsymbol{r}}\otimes\mathrm{n})_0+\rho(\hat{\boldsymbol{r}}\otimes\hat{\boldsymbol{r}}\otimes\mathrm{n})_1+\mathrm{O}(\rho^2),
\end{aligned}
\tag{61}
$$

$$
\begin{aligned}
\mathrm{n}\otimes\hat{\boldsymbol{r}}\otimes\hat{\boldsymbol{r}} &= \hat{\boldsymbol{n}}^0\otimes\boldsymbol{d}_0(\theta)\otimes\boldsymbol{d}_0(\theta)+\rho\begin{bmatrix}\hat{\boldsymbol{n}}^0\otimes\boldsymbol{d}_0(\theta)\otimes\boldsymbol{d}_1(\theta)+\hat{\boldsymbol{n}}^0\otimes\boldsymbol{d}_1(\theta)\otimes\boldsymbol{d}_0(\theta)\\+\hat{\boldsymbol{n}}^1(\theta)\otimes\boldsymbol{d}_0(\theta)\otimes\boldsymbol{d}_0(\theta)\end{bmatrix}+\mathrm{O}(\rho^2)\\
&=(\mathrm{n}\otimes\hat{\boldsymbol{r}}\otimes\hat{\boldsymbol{r}})_0+\rho(\mathrm{n}\otimes\hat{\boldsymbol{r}}\otimes\hat{\boldsymbol{r}})_1+\mathrm{O}(\rho^2),
\end{aligned}
\tag{62}
$$

$$
\begin{aligned}
(\boldsymbol{I}\otimes\mathrm{n})^{213} &= (\boldsymbol{I}\otimes\boldsymbol{n}^0)^{213}+\rho(\boldsymbol{I}\otimes\boldsymbol{n}^1(\theta))^{213}+\mathrm{O}(\rho^2)\\
&=[\boldsymbol{I}\otimes\mathrm{n}]_0^{213}+\rho[\boldsymbol{I}\otimes\mathrm{n}]_1^{213}+\mathrm{O}(\rho^2),
\end{aligned}
\tag{63}
$$

$$
\begin{aligned}
(\boldsymbol{I}\otimes\mathrm{n})^{312} &= (\boldsymbol{I}\otimes\boldsymbol{n}^0)^{312}+\rho(\boldsymbol{I}\otimes\boldsymbol{n}^1(\theta))^{312}+\mathrm{O}(\rho^2)\\
&=[\boldsymbol{I}\otimes\mathrm{n}]_0^{312}+\rho[\boldsymbol{I}\otimes\mathrm{n}]_1^{312}+\mathrm{O}(\rho^2),
\end{aligned}
\tag{64}
$$

$$
\begin{aligned}
(\boldsymbol{I}\otimes\mathrm{n}) &= (\boldsymbol{I}\otimes\boldsymbol{n}^0)+\rho(\boldsymbol{I}\otimes\boldsymbol{n}^1(\theta))+\mathrm{O}(\rho^2)\\
&=[\boldsymbol{I}\otimes\mathrm{n}]_0+\rho[\boldsymbol{I}\otimes\mathrm{n}]_1+\mathrm{O}(\rho^2).
\end{aligned}
\tag{65}
$$

Using Eq. (24), (28), (45) and (50) is obtained Laurent series for $\tilde{\boldsymbol{K}}(\rho,\theta)$:

$$
\tilde{\boldsymbol{K}}(\rho,\theta)=\boldsymbol{U}(\rho,\theta)\left[\mathrm{N}_0^a J_0+\rho\left[\mathrm{N}_0^a J_1(\theta)+\mathrm{N}_1^a(\theta)J_0\right]+\mathrm{O}(\rho^2)\right]\rho=\mathrm{O}(1).
\tag{66}
$$

As would be expected, Eq. (66) is regular, even when $\rho\to 0$. With the aid of Eq. (25), (50), (51), (52), and (58), one has the expression for $\tilde{\boldsymbol{W}}(\rho,\theta)$ and, consequently, for $\tilde{\boldsymbol{W}}_{-1}(\rho,\theta)$

$$
\begin{aligned}
&\tilde{\boldsymbol{W}}(\rho,\theta)=\frac{1}{\rho}\left\{-\frac{1}{8\pi(1-\nu)A^2(\theta)}(1-2\nu)\left[(\boldsymbol{n}_x\otimes\hat{\boldsymbol{r}})_0-(\hat{\boldsymbol{r}}\otimes\boldsymbol{n}_x)_0\right]\mathrm{N}_0^a J_0\right\}+\mathrm{O}(1)\\
&\Rightarrow\tilde{\boldsymbol{W}}_{-1}(\theta)=-\frac{1}{8\pi(1-\nu)A^2(\theta)}(1-2\nu)\left[(\boldsymbol{n}_x\otimes\hat{\boldsymbol{r}})_0-(\hat{\boldsymbol{r}}\otimes\boldsymbol{n}_x)_0\right]\mathrm{N}_0^a J_0.
\end{aligned}
\tag{67}
$$

Using Eq. (26), (53), (54), (57), and (59), it is possible to write the expression for $\tilde{\boldsymbol{D}}_{-1}(\theta)$:

$$
\begin{aligned}
&\tilde{\boldsymbol{D}}(\rho,\theta)=\frac{1}{\rho}\left\{\frac{1}{8\pi(1-\nu)A^2}\left[(1-2\nu)\left[[\boldsymbol{I}\otimes\hat{\boldsymbol{r}}]_0+[\boldsymbol{I}\otimes\hat{\boldsymbol{r}}]_0^{132}-[\hat{\boldsymbol{r}}\otimes\boldsymbol{I}]_0\right]+3[\hat{\boldsymbol{r}}\otimes\hat{\boldsymbol{r}}\otimes\hat{\boldsymbol{r}}]_0\right]\mathrm{N}_0^a J_0\right\}+\mathrm{O}(1)\\
&\Rightarrow\tilde{\boldsymbol{D}}_{-1}(\theta)=\frac{1}{8\pi(1-\nu)A^2}\left\{(1-2\nu)\left[[\boldsymbol{I}\otimes\hat{\boldsymbol{r}}]_0+[\boldsymbol{I}\otimes\hat{\boldsymbol{r}}]_0^{132}-[\hat{\boldsymbol{r}}\otimes\boldsymbol{I}]_0\right]+3[\hat{\boldsymbol{r}}\otimes\hat{\boldsymbol{r}}\otimes\hat{\boldsymbol{r}}]_0\right\}\mathrm{N}_0^a J_0.
\end{aligned}
\tag{68}
$$

Through Eq. (27), (55)-(59) and (61)-(65) can be explained first and second terms of Laurent series:

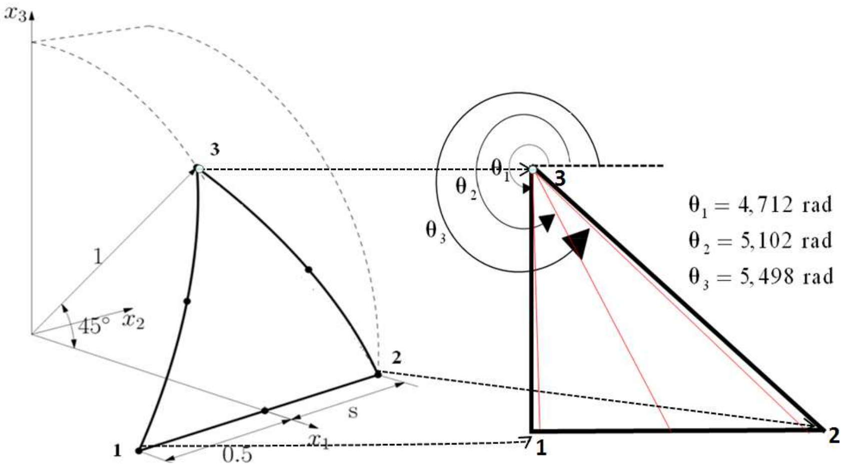

Fig. 2. Curved element and angles to verify the subtraction of singularity.

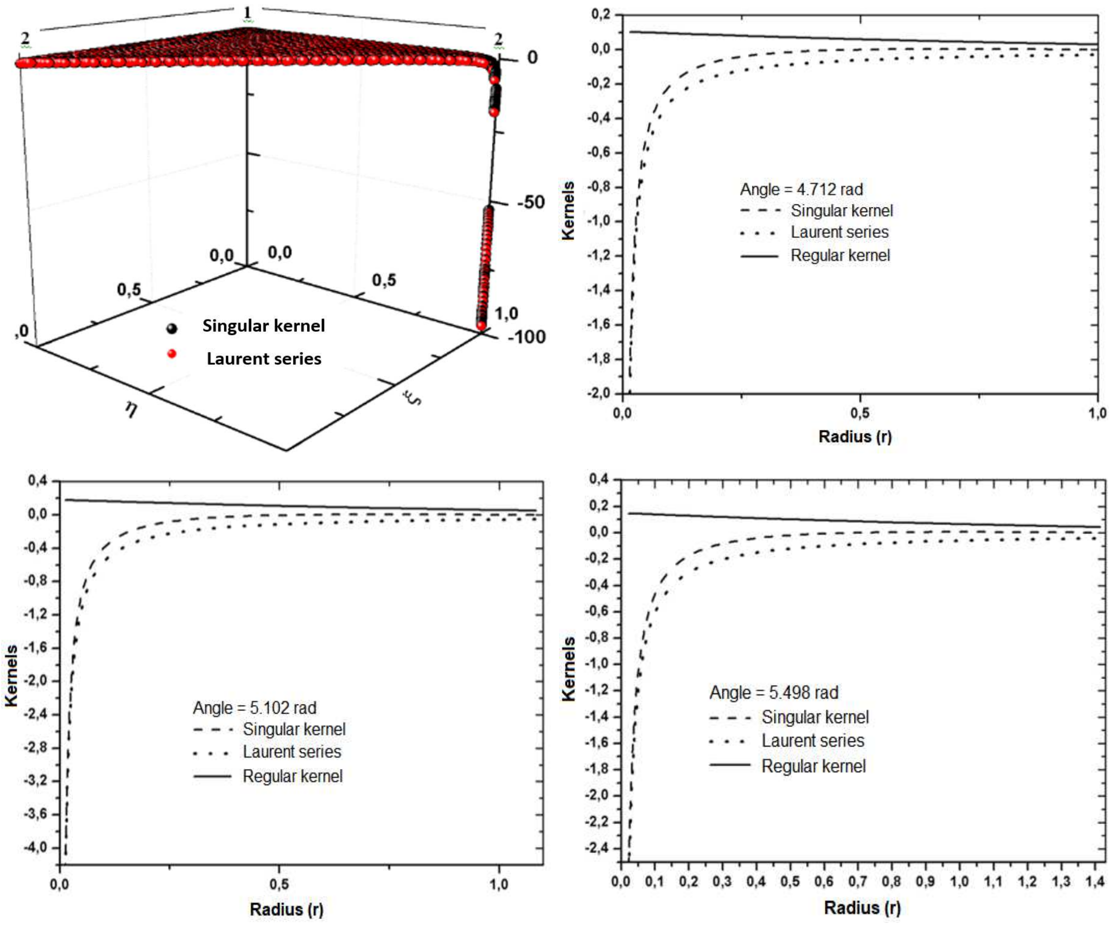

Fig. 3. Singular kernel $\tilde{W}_{31} = T_{31}N^3J$, the first term of Laurent series $\tilde{W}_{-1}$ and the regular kernel; source point at the three-position $(\xi,\eta)=(0,1)$ and $s=0,5$.

$$
\begin{aligned}
\tilde{S}(\rho,\theta) = {} & \frac{1}{\rho^2}\frac{\mu}{4\pi(1-\nu)A^3(\theta)}\begin{bmatrix} 3\nu\left[(\hat{r}\otimes n\otimes\hat{r})_0+(\hat{r}\otimes\hat{r}\otimes n)_0\right] \\ +(1-2\nu)\left[3(n\otimes\hat{r}\otimes\hat{r})_0+(I\otimes n^0)^{213}+(I\otimes n^0)^{312}\right] \\ -(1-4\nu)n^0\otimes I \end{bmatrix} N_0^a J_0 \\
& +\frac{1}{\rho}\frac{\mu}{4\pi(1-\nu)A^3(\theta)}\left\{\begin{bmatrix} N_0^a J_1(\theta) \\ +N_1^a(\theta)J_0 \end{bmatrix}\begin{bmatrix} 3\nu\left[(\hat{r}\otimes n\otimes\hat{r})_0+(\hat{r}\otimes\hat{r}\otimes n)_0\right] \\ +(1-2\nu)\left[3(n\otimes\hat{r}\otimes\hat{r})_0+(I\otimes\hat{n}_x^0)^{213}+(I\otimes\hat{n}_x^0)^{312}\right] \\ -(1-4\nu)\hat{n}_x^0\otimes I \end{bmatrix}\right.
\end{aligned}
\tag{69}
$$

$$
+\mathrm{N}_0^a J_0 \left[\begin{array}{l} 3\nu\left[(\hat{\boldsymbol{r}}\otimes \mathrm{n}\otimes \hat{\boldsymbol{r}})_1+(\hat{\boldsymbol{r}}\otimes \hat{\boldsymbol{r}}\otimes \mathrm{n})_1\right] \\ +3(\hat{\boldsymbol{n}}_x\cdot \hat{\boldsymbol{r}})_1\left[\begin{array}{l}(1-2\nu)(\hat{\boldsymbol{r}}\otimes \boldsymbol{I})_0+\nu\left[[\boldsymbol{I}\otimes\hat{\boldsymbol{r}}]_0^{213}+[\boldsymbol{I}\otimes\hat{\boldsymbol{r}}]_0^{312}\right] \\ -5(\hat{\boldsymbol{r}}\otimes \hat{\boldsymbol{r}}\otimes \hat{\boldsymbol{r}})_0\end{array}\right] \\ +(1-2\nu)\left[3(\mathrm{n}\otimes \hat{\boldsymbol{r}}\otimes \hat{\boldsymbol{r}})_1+(\boldsymbol{I}\otimes \mathrm{n})_1^{213}+(\boldsymbol{I}\otimes \mathrm{n})_1^{312}\right]-(1-4\nu)(\mathrm{n}\otimes \boldsymbol{I})_1 \\ -3\dfrac{(\boldsymbol{A}\cdot\boldsymbol{B})}{\mathrm{A}^2}\left[\begin{array}{l}3\nu\left[(\hat{\boldsymbol{r}}\otimes \mathrm{n}\otimes \hat{\boldsymbol{r}})_0+(\hat{\boldsymbol{r}}\otimes \hat{\boldsymbol{r}}\otimes \mathrm{n})_0\right] \\ +(1-2\nu)\left[3(\mathrm{n}\otimes \hat{\boldsymbol{r}}\otimes \hat{\boldsymbol{r}})_0+(\boldsymbol{I}\otimes \mathrm{n})_0^{213}+(\boldsymbol{I}\otimes \mathrm{n})_0^{312}\right] \\ -(1-4\nu)(\mathrm{n}\otimes \boldsymbol{I})_0\end{array}\right]\end{array}\right]\Bigg\} + O(1).
$$

$$
\Rightarrow \tilde{\boldsymbol{S}}_{-2}(\theta)=\frac{\mu}{4\pi(1-\nu)\mathrm{A}^3(\theta)}\left[3\nu\left[(\hat{\boldsymbol{r}}\otimes \mathrm{n}\otimes \hat{\boldsymbol{r}})_0+(\hat{\boldsymbol{r}}\otimes \hat{\boldsymbol{r}}\otimes \mathrm{n})_0\right]+(1-2\nu)\left[3(\mathrm{n}\otimes \hat{\boldsymbol{r}}\otimes \hat{\boldsymbol{r}})_0+\left(\boldsymbol{I}\otimes \boldsymbol{n}^0\right)^{213}+\left(\boldsymbol{I}\otimes \boldsymbol{n}^0\right)^{312}\right]-(1-4\nu)\boldsymbol{n}^0\otimes \boldsymbol{I}\right]\mathrm{N}_0^a J_0,
$$

$$
\Rightarrow \tilde{\boldsymbol{S}}_{-1}(\theta)=\frac{\mu}{4\pi(1-\nu)\mathrm{A}^3(\theta)}\left\{\begin{array}{l}\left[\mathrm{N}_0^a J_1(\theta)+\mathrm{N}_1^a(\theta)J_0\right]\left[3\nu\left[(\hat{\boldsymbol{r}}\otimes \mathrm{n}\otimes \hat{\boldsymbol{r}})_0+(\hat{\boldsymbol{r}}\otimes \hat{\boldsymbol{r}}\otimes \mathrm{n})_0\right]+(1-2\nu)\left[3(\mathrm{n}\otimes \hat{\boldsymbol{r}}\otimes \hat{\boldsymbol{r}})_0+\left(\boldsymbol{I}\otimes \hat{\boldsymbol{n}}_x^0\right)^{213}+\left(\boldsymbol{I}\otimes \hat{\boldsymbol{n}}_x^0\right)^{312}\right]-(1-4\nu)\hat{\boldsymbol{n}}_x^0\otimes \boldsymbol{I}\right] \\ +\mathrm{N}_0^a J_0\left[\begin{array}{l}3\nu\left[(\hat{\boldsymbol{r}}\otimes \mathrm{n}\otimes \hat{\boldsymbol{r}})_1+(\hat{\boldsymbol{r}}\otimes \hat{\boldsymbol{r}}\otimes \mathrm{n})_1\right]+3(\hat{\boldsymbol{n}}_x\cdot \hat{\boldsymbol{r}})_1\left[(1-2\nu)(\hat{\boldsymbol{r}}\otimes \boldsymbol{I})_0+\nu\left[[\boldsymbol{I}\otimes\hat{\boldsymbol{r}}]_0^{213}+[\boldsymbol{I}\otimes\hat{\boldsymbol{r}}]_0^{312}\right]-5(\hat{\boldsymbol{r}}\otimes \hat{\boldsymbol{r}}\otimes \hat{\boldsymbol{r}})_0\right] \\ +(1-2\nu)\left[3(\mathrm{n}\otimes \hat{\boldsymbol{r}}\otimes \hat{\boldsymbol{r}})_1+(\boldsymbol{I}\otimes \mathrm{n})_1^{213}+(\boldsymbol{I}\otimes \mathrm{n})_1^{312}\right]-(1-4\nu)(\mathrm{n}\otimes \boldsymbol{I})_1 \\ -3\dfrac{(\boldsymbol{A}\cdot\boldsymbol{B})}{\mathrm{A}^2}\left[3\nu\left[(\hat{\boldsymbol{r}}\otimes \mathrm{n}\otimes \hat{\boldsymbol{r}})_0+(\hat{\boldsymbol{r}}\otimes \hat{\boldsymbol{r}}\otimes \mathrm{n})_0\right]+(1-2\nu)\left[3(\mathrm{n}\otimes \hat{\boldsymbol{r}}\otimes \hat{\boldsymbol{r}})_0+(\boldsymbol{I}\otimes \mathrm{n})_0^{213}+(\boldsymbol{I}\otimes \mathrm{n})_0^{312}\right]-(1-4\nu)(\mathrm{n}\otimes \boldsymbol{I})_0\right]\end{array}\right]\end{array}\right\}. \tag{70}
$$

It is important to note that the integral equations (25)-(27) are regulars, and then these are developed numerically by standard quadrature formulas. Some regular kernels present in equations (25)-(27) are shown in Figures 3-8. The singular kernels $\tilde{\boldsymbol{W}}_{ij}$, $\tilde{\boldsymbol{D}}_{kij}$, and $\tilde{\boldsymbol{S}}_{kij}$ (dashed line) and the corresponding singular terms of Laurent series (see Eq. (67)-(70), dotted line) are also in each of the figures. The regularized kernel is obtained by subtracting the singular terms of Eq. (17) by the terms of Eq. (29)-(31).

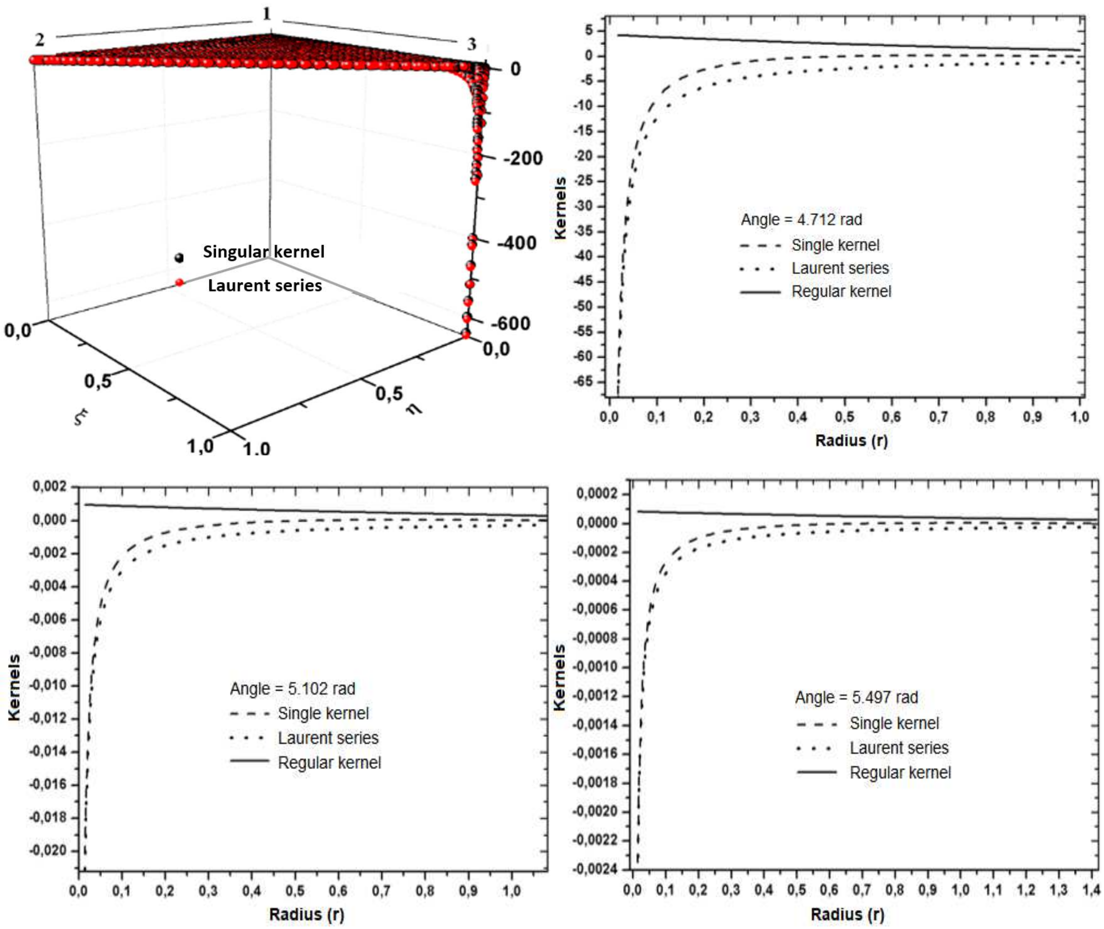

Fig. 4. Singular kernel $\tilde{W}_{31}=\boldsymbol{T}_{31}\mathrm{N}^3 J$, the first term of Laurent series $\tilde{W}_{-1}$ and the regular kernel; source point at the three-position, $(\xi,\eta)=(0,1)$, and $\mathrm{s}=40$.

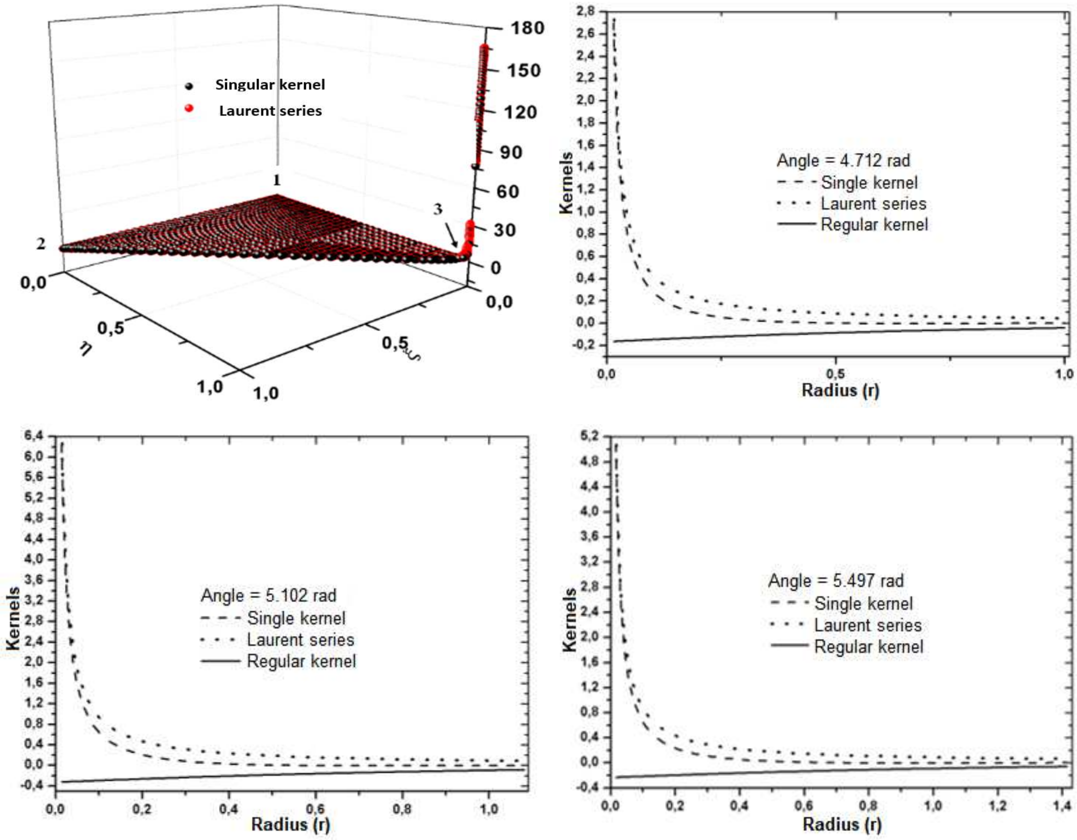

Fig. 5. Singular kernel $\tilde{\boldsymbol{D}}_{111} = \boldsymbol{D}_{111} N^3 J$, the first term of Laurent series $\tilde{\boldsymbol{D}}_{-1}$ and the regular kernel; source point at the three-position, $(\xi,\eta) = (0,1)$, and $s = 0,5$.

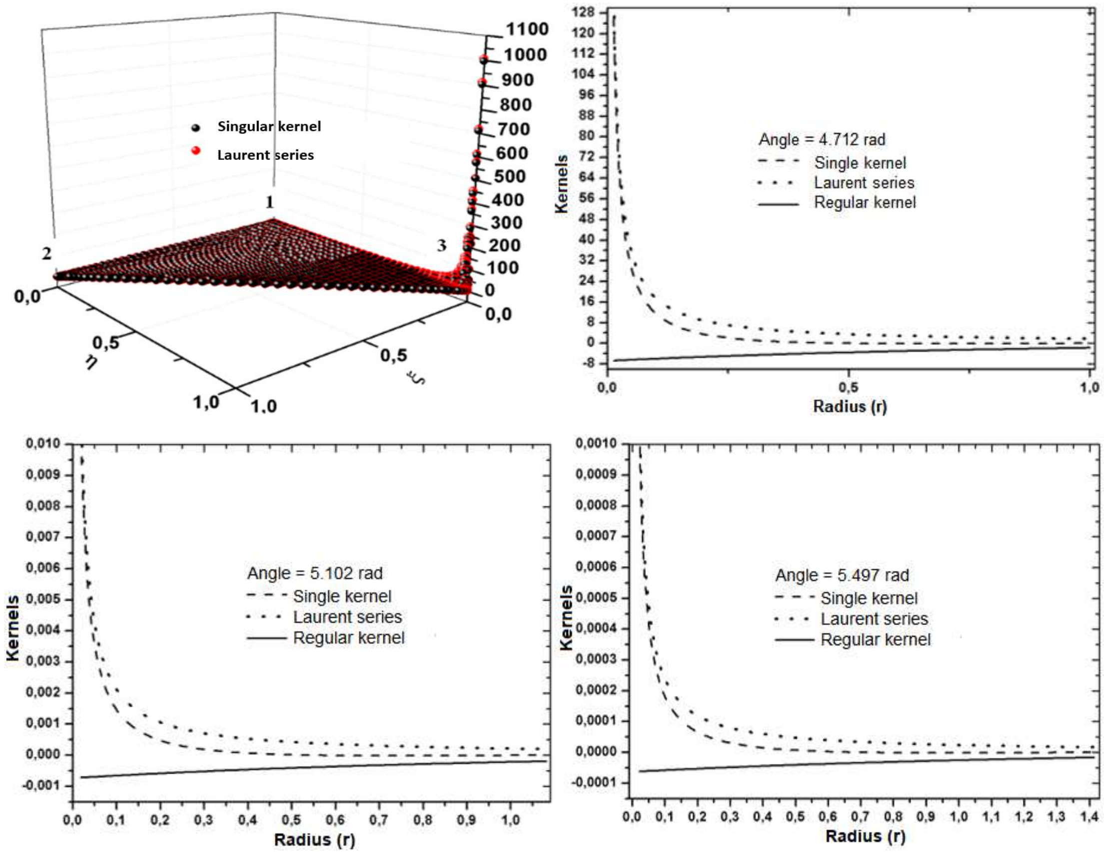

Fig. 6. Singular kernel $\tilde{\boldsymbol{D}}_{111} = \boldsymbol{D}_{111} N^3 J$, the first term of Laurent series $\tilde{\boldsymbol{D}}_{-1}$ and the regular kernel; source point at the three-position, $(\xi,\eta) = (0,1)$, and $s = 40$.

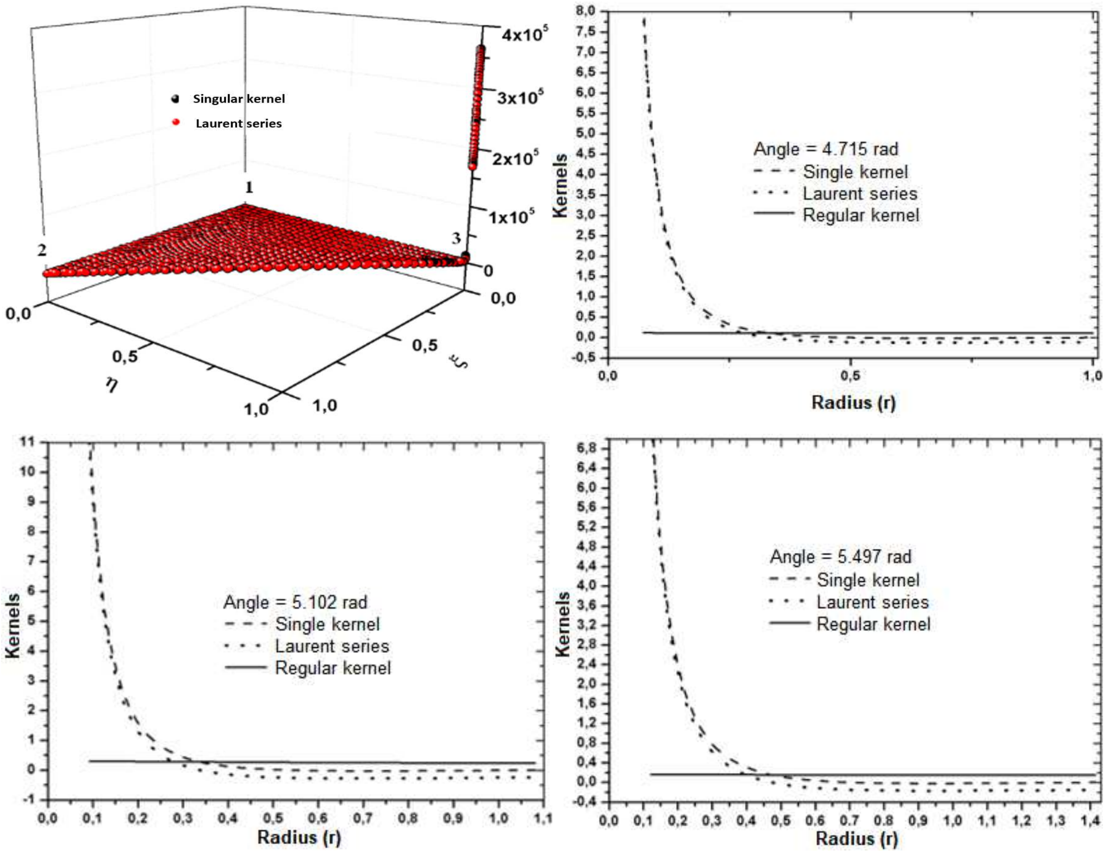

Fig. 7. Singular kernel $\tilde{S}_{111} = S_{111}N^3J$, the first two terms of the Laurent series $\tilde{S}_{-1}$, $\tilde{S}_{-2}$ and the regular kernel; source point at the three-position $(\xi,\eta) = (0,1)$, and s = 0,5 .

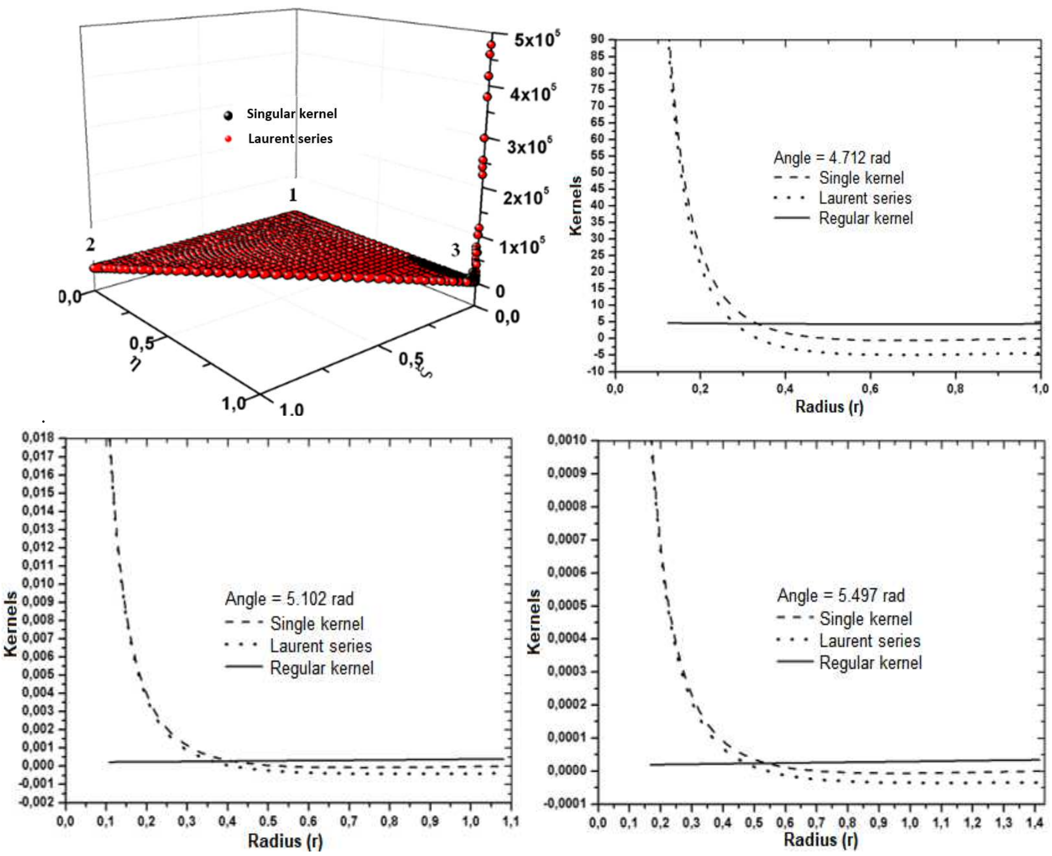

Fig. 8. Singular kernel $\tilde{S}_{111} = S_{111}N^3J$, the first two terms of the Laurent series $\tilde{S}_{-1}$, $\tilde{S}_{-2}$ and the regular kernel; source point at the three-position $(\xi,\eta) = (0,1)$, and s = 40 .

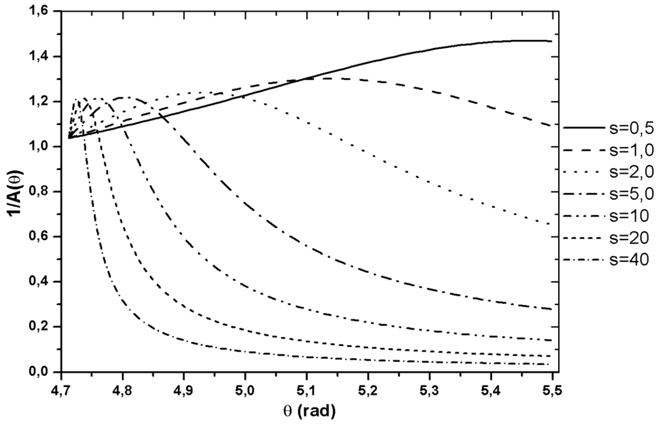

Fig. 9. $1/A(\theta)$ graph for various s values, with source point at the 3 positions in Fig (1).

The results in Fig. 3-8 are for a curved triangular element shown in Fig. 2. The behavior of the singularity treatment of the first terms on the right side of Eqs. (25)-(27) are shown in Figures 3-8, as the s parameter varies, i. e., as the curved element becomes distorted. It can be seen that the distortion of the element weakly influences the subtraction of singularity to the regularized kernels in the radial direction, even when the term $1/A(\theta)$ varies rapidly as the value of the parameter s increases, i.e., the term $1/A(\theta)$, in this circumstance, presents characteristics of near singularity, which can be seen in Fig. 9. However, care must be taken in performing the numerical integrations of the second term of Eq. (25)-(27) when the element becomes much distorted. This careful nor observed by Guiggiani et al. [4] should be considered because elements with significant distortion appear the effect of the boundary layer (nearly singularity) in these integrations, which can deteriorate the numerical calculation of integral kernels.

Finally, to make possible the calculation of the integrals in Eq. (25)-(27), the expressions of $\beta(\theta)$ and $\gamma(\theta)$ parameters are explained. The contour of the neighborhood, S_ϵ, for point source with radius ϵ, is given by Eq. (71),

$$\epsilon = r. \tag{71}$$

Using Eq. (40) and (71), the parametric plane written in polar coordinates can be written by

$$\epsilon = r = \rho A(\theta)\left[1 + \rho\frac{(\boldsymbol{A}(\theta)\cdot\boldsymbol{B}(\theta))}{A^2(\theta)}\right] + O(\rho^3). \tag{72}$$

Applying Eq. (42) in the above equation, it is possible to obtain the expansion in power series, in ϵ, for the equation in polar coordinates of the σ_ϵ contour, the image of S_ϵ,

$$\rho = \alpha(\epsilon,\theta) = \frac{\epsilon}{A(\theta)} - \epsilon^2\frac{\boldsymbol{A}(\theta)\cdot\boldsymbol{B}(\theta)}{A^4(\theta)} + O(\epsilon^3). \tag{73}$$

From the comparison between Eq. (73) and Eq. (18), it is concluded that

$$\beta(\theta) = \frac{1}{A(\theta)}, \quad \gamma(\theta) = \frac{\boldsymbol{A}(\theta)\cdot\boldsymbol{B}(\theta)}{A^4(\theta)}. \tag{74}$$

4. Conclusion

More efficient and highly accurate procedures are crucial to the high order Boundary Element Method. In Guiggiani et al. (1992), a unified framework has been proposed to treat the BEM's singular kernels of various orders. This method is based on the transformation into polar coordinates, widely used to treat singular integral to the boundary elements. This paper developed explicit expressions for the Laurent series's singular terms for the integral equations of the BEM applied to three-dimensional elastostatic problems. After writing the Laurent series's explicit form, one verifies that the accuracy of this series in the radial direction has excellent agreement with the singular kernels of the BEM. Conversely, when the analysis is performed in the angular direction, it can be observed that as the parameter s is varied, i.e., as the curved element becomes distorted, the term $1/A(\theta)$ undergoes the boundary layer (nearly singularity) (see Fig. 9). This boundary layer effect can quickly deteriorate the accuracy of singularity's subtraction as the last integral term in Eq. (27) becomes predominant. However, Guiggiani et al. (1992) did not report this possibility of deterioration of integration. Thus, it is necessary to more carefully when the integration is performed in the θ direction (angular direction), and not only in the radial direction when distorted curved elements are used.

Author Contributions

L. F. D. Leite developed some analytical expressions; R. S. De Melo elaborated the graphics for the example of validation; F. C. Da Rocha planned the project, suggested the theoretical approach, and examined the analytical expressions and numerical results. The manuscript was written through the contribution of all authors. All authors discussed the results, reviewed, and approved the final version of the manuscript.

Acknowledgments

The authors would like to acknowledge the Federal University of Sergipe, through the institutional program PIBIC, for their support in carrying out this work.

Conflict of Interest

The authors declared no potential conflicts of interest with respect to the research, authorship, and publication of this article.

Funding

The authors received financial support from the Coordenação de Aperfeiçoamento de Pessoal de Nível Superior - Brazil (CAPES) - Finance code 001.

Nomenclature

V	Problem domain	ς	Global numbering
S	Problem boundary	$\mathbf{C}, \bar{\mathbf{C}}, \mathbf{B}^{123}$	Tensors that depend only on local geometry
S^A	Augmented problem boundary	N^a, M^c	Shape functions
S_ε	Original boundary removed	ξ	Dimensionless local coordinate
S_ε^+	Portion of the inserted boundary	$u^a{}_e$	Nodal displacements of the element e
S_S	Region into S containing the singular point	ρ	Radial coordinate
D	Cartesian dimension	θ	Angular coordinate
μ	Shear modulus of elasticity	ξ_1, ξ_2	Parametric coordinates
ν	Poisson's ratio	η	Parametric image of the singular point
E	Young's modulus	R_S	Parametric domain
β	Level's singularities	J	Jacobian of transformation
$\mathbf{u}$	Displacements	$\hat{\rho}(\theta)$	Polar coordinate of the outer boundary in R_S
$\mathbf{t}$	Tractions	F_{-1}, F_{-2}	Laurent series coefficients
$\mathbf{b}$	Body forces	$\alpha(\epsilon,\theta)$	Region surrounding the singular point
X	Field point in domain	$A(e)$	Number of nodes in the element
x	Field point on boundary	N_e	Number of elements
Y	Source point in domain	L	Total number of nodes
$\mathbf{U}, \mathbf{T}, \mathbf{D}, \mathbf{S}$	Fundamental solutions	x^c	Nodal coordinate
$\boldsymbol{\sigma}$	Stress tensor	$\tilde{W}_{-1}, \tilde{D}_{-1}, \tilde{S}_{-1}$	first terms of the Laurent series
$\mathbf{I}$	Second order identity tensor	$\tilde{D}_{-2}, \tilde{S}_{-2}$	Second terms of the Laurent series
$\mathbf{n}$	Normal vector	$\tilde{K}$	Regular kernel
$\mathbf{r}$	Distance between field and source points	$\tilde{W}$	Singular Kernel
r	Module of distance vector	$\tilde{D}, \tilde{S}$	Hypersingular kernel
$\hat{r} = \mathbf{r}/r$	Unit distance vector	$\boldsymbol{H}_\varsigma^k, \boldsymbol{G}_\varsigma^k, \bar{\boldsymbol{H}}_\varsigma^k, \bar{\boldsymbol{G}}_\varsigma^k$	Matrices of BEM coefficients.

References

[1] Canino, L. F., Ottush, J. J., Stalzer, M. A., Numerical solution of the Helmhotz equation in 2D and 3D using a high-order Nyström discretization, *Journal of Computational Physics*, 144, 1998, 627-633.
[2] Rjasanow, S., Weggler, L., Accelerated high order BEM for Maxwell problems, *Computational Mechanics*, 51, 2013, 431-441.
[3] Gao, X. W., Davies, T. G., *Boundary Element Programming in Mechanics*, Cambridge University Press, 2002.
[4] Guiggiani, M., Krishnasamy, G., Rudolphi, T. J., Rizzo, F. J., A general algorithm for the numerical solution of hypersingular boundary integral equations, *ASME Journal of Applied Mechanics*, 52, 1992, 604-614.
[5] Carley, M., Numerical quadratures for singular and hypersingular integrals in boundary element methods, *SIAM Journal on scientific computing*, 29, 2007, 1207-1216.
[6] Johnston, B. M., Johnston, P. R., A comparison of transformation methods for evaluating two-dimensional weakly singular integrals, *International Journal for Numerical Methods in Engineering*, 56, 2003, 589-607.
[7] Gao, X. W., An effective method for numerical evaluation of general 2D and 3D high order singular boundary integrals, *Computer Methods in Applied Mechanics and Engineering*, 199, 2010, 2856-2864.
[8] Aliabadi, M. H., *The Boundary Element Method: applications in solids and structures*, Wiley, 2002.
[9] Abramowitz, M., Stegun, I. A., *Handbook of Mathematical Functions with Formulas, Graphs, and Mathematical Tables*, Dover, 1972.

ORCID iD

Leonardo Fellipe Prado Leite https://orcid.org/0000-0002-1854-1425
Rodrigo Souza de Melo https://orcid.org/0000-0003-0346-1841
Fabio Carlos da Rocha https://orcid.org/0000-0002-1054-3397

How to cite this article: Prado Leite L.F., de Melo R.S., da Rocha F.C. Analytical expressions for the singularities treatment in the three-dimensional elastostatic Boundary Element Method, *J. Appl. Comput. Mech.*, 7(2), 2021, 739–751.
https://doi.org/10.22055/JACM.2020.35017.2539